Proceedings of the 20th International Conference on Soil Mechanics and Geotechnical Engineering– Rahman and Jaksa (Eds)

Experimental and numerical assessment of fabric anisotropy using multi-orientation shear wave velocity measurements

Évaluation expérimentale et numérique de l'anisotropie de la texture au moyen de mesures multidirectionnelles de la vitesse d'ondes de cisaillement.

Mandeep Singh Basson & Alejandro Martinez
Department of Civil and Environmental Engineering, University of California Davis, USA, mbasson@ucdavis.edu

ABSTRACT: The soil fabric is made up of the arrangement of soil particles and inter-particle interactions, which impacts the behavior of granular soils and can lead to anisotropic soil characteristics and behavior. This paper provides the results of an experimental and numerical investigation aimed at developing an indirect method to measure the fabric of coarse-grained soils using multi-orientation measurements of shear wave velocity, V_s. V_s measurements are obtained on specimens prepared with varying degrees of fabric and stress anisotropy. The results indicate that the changes in contact fabric affect the stiffness anisotropy as shown by the angular distribution of measured V_s. Results during K_0 compression highlight the stress anisotropy, with maximum V_s aligning with the major principal stress direction. Isotropic compression results highlight the effect of particle shape orientation, where the maximum Vs aligns with the direction with long axis orientation. The ability to measure V_s experimentally and numerically is shown to provide an indirect estimation of contact fabric and link the physical and numerical modeling of coarse-grained soils.

RÉSUMÉ : Cet article présente les résultats d'une étude expérimentale et numérique visant à élaborer une méthode de mesure indirecte de la structure de sols granulaires au moyen de mesures multidirectionnelles de la vitesse d'ondes de cisaillement (V_s). Les mesures de Vs sont obte-nues sur des échantillons préparés avec différents niveaux d'anisotropie de texture et de contrainte. Les résultats indiquent que les variations de la texture de contact influencent l'anisotropie de rigidité comme en atteste la distribution angulaire des Vs mesurées. Les ré-sultats pendant la compression K_0 mettent en évidence l'anisotropie de contrainte, la Vs maximale correspondant à la direction de contrainte principale majeure. Les résultats de la compression isotrope font ressortir l'incidence de l'orientation de la forme des particules, la V_s maximale correspondant à l'orientation de l'axe long. La mesure numérique et expérimentale de la V_s permet d'obtenir une estimation indirecte de la structure de contact et de faire le lien entre la modélisation physique et numérique des sols granulaires

KEYWORDS: Granular materials, Fabric anisotropy, Shear wave velocity, DEM.

1 INTRODUCTION

At a micro scale, coarse-grained soils consist of an arrangement of discrete particles. The particulate nature of granular soils can lead to anisotropy in strength and stiffness (Oda 1972, Oda et al. 1982). This anisotropy can be due to the (i) anisotropy in inherent fabric, which consists of the arrangement of particles, contacts, and voids and is a result of deposition and post-deposition processes as well as to the soil gradation and particle shape and (ii) stress anisotropy resulting from the state of stresses which affects the forces transmitted at interparticle contacts (Rothenburg & Bathurst 1989, Stokoe & Santamarina 2006, Cha et al. 2014, , Li & Zeng 2014, Fu & Dafalias 2015, Basson & Martinez 2020, Otsubo et al. 2020) Although researchers have employed advanced imaging (e.g. X-ray CT) and computational (e.g. discrete element modeling (DEM)) techniques to assess the anisotropy in soil behavior, experimental measurement of soil fabric remains a challenge due to the difficulties involved in obtaining experimental particle-level measurements.

The shear wave velocity (V_s) of a soil depends on its shear stiffness at low strain (G_{max}). V_s is an essential parameter in soil characterization, testing, and design because it can be measured in the field, laboratory, and numerical simulation, and provides a link between macro, meso, and micro scale behavior of granular soils. The propagation of shear waves through the soil medium is a low-strain perturbation that does not create plastic deformations or modify the fabric. As a result, V_s measurements provide a reproducible and non-destructive way of characterizing soils and estimating G_{max}. Experimentally, Bender Elements (BEs) can be used as actuators and receivers to measure V_s in soil specimens and estimate the anisotropy in shear stiffness (e.g. Viggiani & Atkinson 1995, Cascante & Santamarina 1996, Arulnathan et al. 1998, Lee & Santamarina 2005, Cho et al. 2006, Otsubo et al. 2018,2020).

Investigations have used DEM to obtain V_s measurements to explore the dependency shear stiffness anisotropy on the state of stresses and on the inherent soil fabric (e.g. O'Donovan et al. 2016, Mital et al. 2019, Otsubo et al. 2020). The results of these investigations suggest that the anisotropy in G_{max} and V_s is related to the anisotropy in fabric. The goal of the investigation presented herein is to develop a method to estimate the fabric anisotropy experimentally. To do so, a multi-bender element system has been developed in which BE pairs are used to measure V_s in different directions (0 to 90°) and orientations (horizontally and vertically polarized waves) in specimens subjected to isotropic and K_0 compression states of stresses. The granular materials tested in this new multi-BE system include glass beads and sub-angular quartz sands. To validate the experimental setup, a DEM model was built in which V_s measurements can also be obtained in different directions and orientations in assemblies composed of spherical and elongated particles. In this paper, both experimental and numerical methods are used to construct polar histograms of shear wave velocity measurements.

2 METHODOLOGY

2.1 Notations of shear wave velocities

Three types of shear waves (VH, HV and HH) were utilized in this study to investigate the effect of fabric anisotropy on the stiffness of the specimen. These shear waves follow the widely used notation in literature, where the first letter denotes the wave propagation direction and the second letter denotes the particle motion direction (Lee & Santamarina 2005, Stokoe & Santamarina 2006). For example, the VH wave is a vertically propagating shear wave with particles moving in the horizontal direction. The shear velocity magnitude for these waves is

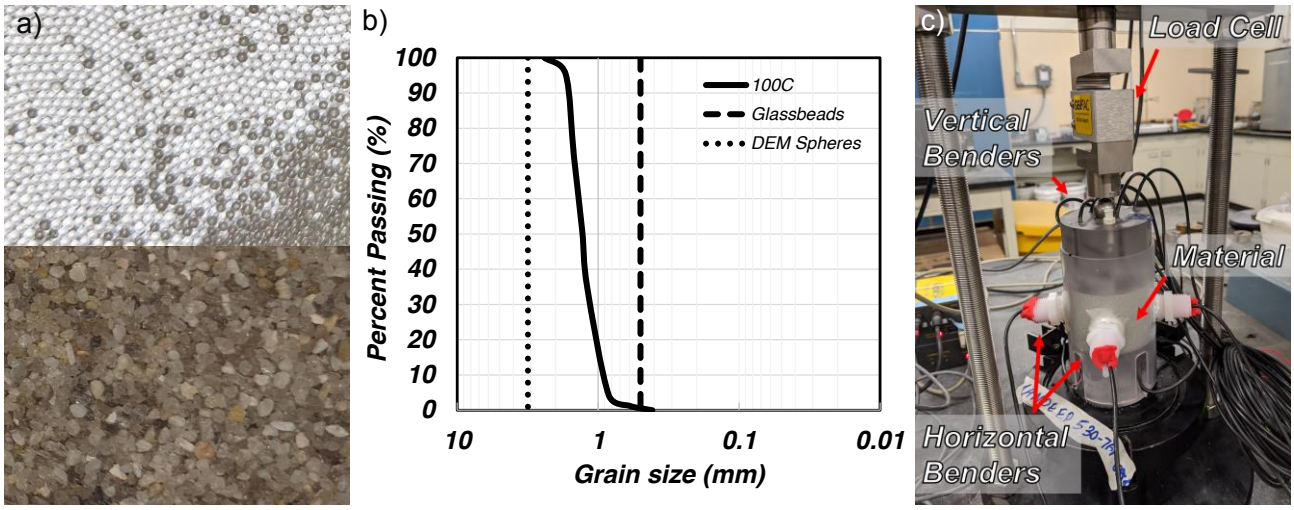

Figure 1. Experimental setup; (a) glass beads and 100C sand, (b) grain size distributions for different materials, (c) setup for K_0 compression

denoted as V_{VH}, V_{HV} and V_{HH}, respectively. Measurements were also obtained at different inclined orientations between the vertical and horizontal directions to construct an angular distribution of V_s. These inclined orientations were part of angular sweeps starting from the vertical orientation and ending at the horizontal orientation. Two sweeps were performed using the above notation, one starting from the VH direction and ending in the HV direction (VH-HV sweep) and the other starting from the VH direction and ending in the HH direction (VH-HH sweep).

2.2 Experimental Setup

2.2.1 Materials and sample preparation

Two materials were tested in the multi-BE system to explore the effect of particle shape and corresponding fabric on the V_s angular variation (Figure 1(a)). Mono-sized glass beads with a diameter of 0.5 mm were used to produce samples with negligible fabric anisotropy. Poorly graded 100C sand sourced from the Cape May Formation near Mauricetown, New Jersey, was used as the natural sand material. This sand has a mean particle size, D_{50}, of 1.31 mm, coefficient of uniformity, C_u, of 1.54, coefficient of curvature, C_c, of 1.02, particle roundness of 0.60 and particle sphericity of 0.77. More details about this soil are presented in Sturm (2019). The grain size distribution of the tested materials is provided in Figure 1(b).

Various sample preparation techniques produce specimens with different internal fabric, which has a considerable effect on the macroscopic response (e.g. Roesler 1979, Rothenburg & Bathurst 1989, Basson & Martinez 2020). The specimen of glass beads and 100C were prepared using the pluviation method for which oven-dried particles were pluviated into the specimen mold from a constant height for both isotropic and K_0 compression tests. Pluviation can produce fabric anisotropy in the specimens due to the tendency of the longest axis of the particles to aligning in the horizontal direction. Once the specimens reached a height of about 40 mm, the top cap was inserted into the mold. For isotropic compression tests, the specimens were formed inside latex membranes and vacuum was applied to produce mean effective stress values of 20, 40, and 60 kPa. For K_0 compression tests, the specimens were formed inside a rigid-wall mold and the top cap with an attached load cell was displaced downward to achieve vertical effective stresses of 20, 40, and 60 kPa (Figure 1c).

2.2.2 Bender Element configuration

In the multi-BE system, five pairs of bender elements were mounted on the top and bottom caps such that their orientations were (from the horizontal) 90˚ (vertical, VH), 75˚, 65˚, 55˚ and 50˚. The bender elements consisted of piezoelectric actuators coated with two layers of epoxy raisin. The BEs were embedded in polycarbonate end caps with a diameter and height of 71mm and 50mm, respectively. More details about these inclined bender elements are provided in Basson et al. (2021). Two additional pairs of bender elements were used to measure V_s in the horizontal direction in the HV and HH orientations. For the isotropic compression tests, the horizontal bender elements were glued to the membrane with a slit in the middle to provide direct contact between the bender elements and the soil. For the K_0 compression tests, the horizontal bender elements were embedded in the polycarbonate mold, as shown in Figure 1c. Due to limited workable space on the end caps, the inclined BEs could only provide V_s values for the VH to HV sweep, with the addition of one V_s measurement in the HH direction.

A single sinusoidal excitation with a voltage of 4.5 V and a frequency of 5 kHz was sent through the BEs embedded in the top cap and received through the BEs embedded in the bottom cap. Similar excitation was sent through one side of the horizontal BE pair and received on the other side. The received signal was first filtered using a Butterworth filter, boosted with a gain of 20, and then fed into an oscilloscope (PicoScope) for analysis. Noise was filtered through the filtering system, and a final clean signal was used for the determination of first arrival times which were then used to determine shear wave velocities.

2.3 Numerical Setup

2.3.1 Materials and sample preparation

The open-source DEM code YADE was used in this study. Specimens consisting of mono-sized spherical particles of 3.15 mm diameter were created to simulate conditions similar to the specimen of glass beads (Figure 2a). Other specimens were created using elongated particles made of three clumped mono-sized spheres to introduce fabric anisotropy in the specimen (Figure 2b)). The Hertz-Mindlin contact law was used to simulate the contact interactions, with a Young's modulus value of 70 GPa, Poisson's ratio of 0.3 and a friction coefficient of 0.1 during sample preparation. The damping coefficient was kept at a value of 0.01 throughout the sample preparation, loading, and wave propagation phases (Moraille et al. 2006). This damping coefficient was briefly increased to 0.5, and the specimen was cycled to ensure negligible particle motions before the wave propagation phase. To simulate the dissipation of non-physical vibrations during wave propagation, the friction coefficient was increased to 0.5. This process ensures elastic response during

wave propagation and removes any movements due to particle sliding (Madanimo et al. 2008).

An effort was made to recreate experimental sample preparation techniques in the numerical simulations to produce similar variations in fabric anisotropy. The specimen with spherical particles and isotropic fabric specimen was prepared by isotropically compressing a cloud of non-contacting particles using periodic boundaries until it reached dimensions of 30 cm by 30 cm by 30 cm, and a mean effective stress of 10 kPa. A pluviation process was recreated for the specimens with elongated clumps to get an initial anisotropy in the fabric. During pluviation, a layer of particles about four diameters thick was dropped in a rigid-walled square container. During the settlement of the particles, rotation was observed such that the longer dimension axis of the particles tended to align in the horizontal direction. This preferential long-axis orientation creates an initial anisotropy in the sample. This layered pluviation was repeated until the specimen size reached 30 cm by 30 cm by 30 cm. The rigid walls were then replaced by periodic boundaries, and the sample was compressed to a mean effective stress of 10 kPa.

These specimens were either compressed isotropically to a mean effective stress of 20, 40 and 60 kPa by equal compression on all sides, or to mean effective stresses of 20, 40, and 60 kPa under K_0 compression by compressing from the top and fixing the all the sides and the bottom. The applied strain rate was kept low enough to keep the Inertial Number (I) less than 10^{-4} during sample preparation, loading and wave propagation phases. The unbalanced forces were kept lower than 10^{-3} during the loading phase.

2.3.2 Bender Element configuration

The numerical transmitting and receiving bender elements were created using thin rectangular layers of particles, as previously implemented by Ning et al. 2015, Otsubo & Sullivan 2018. Shear waves were generated by applying an excitation, in the form of a single sinusoidal displacement with a pre-defined amplitude, to a thin layer of particles towards the top end. This amplitude was varied between 10^{-7} m to 10^{-5} m to keep the unbalanced forces below 10^{-3}. The frequency of this excitation was selected as 5 kHz after a parametric study was done to identify the resonant frequency of the specimen, as previously done by Ning & Evans 2013, Mital et al. 2019, and Otsubo et al. 2020. DEM simulations provide an ability to track each particle's displacements and velocities to receive the wave at multiple locations throughout the specimen. The shear wave was received at ten equidistant receiving locations consisting of similar thin layers of particles. The displacement of these receiver particles was averaged to produce an overall received signal per layer. These rectangular transmitting and receiving layers were 15 cm by 15 cm by 2.5 particle diameters. Similar to the experiments, this configuration creates a spherical wave front with the added advantage of reduction in P-wave interference (Lee & Santamarina 2005, Otsubo et al. 2020) (Figures 2(c,d,e,f)). These numerical bender elements were inclined to provide measurements between the range of -90˚ to 90˚ (from horizontal) in 15˚ increments.

3 RESULTS

3.1 Travel time estimation

Shear wave propagation in granular materials is a complex physical phenomenon that causes significant uncertainty in signal interpretation, particularly in determining wave travel times (Viggiani & Atkinson 1995, Arulnathan et al. 1998, Lee & Santamarina 2005, Ogino et al. 2015). In this experiment, travel times were calculated by visually identifying deflection in the received signal. Figure 3 and Figure 4 shows the filtered transmitted and received signal for experiments and numerical

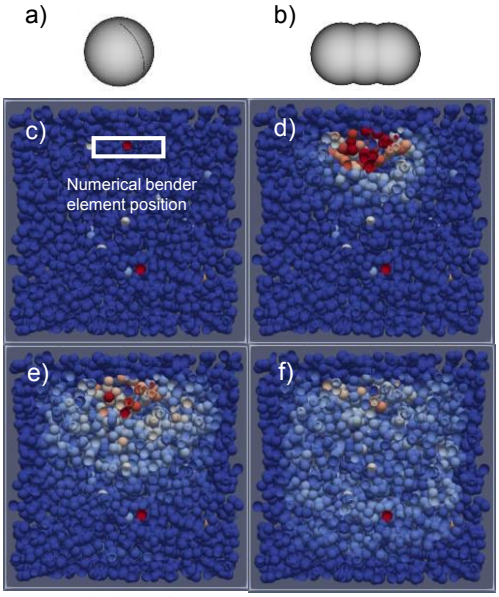

Figure 2. Details about the numerical setup; (a) spheres, (b) clumps, (c, d,e,f) particle velocities at different stages during the simulation showin g the propagation of shear wave.

simulations, respectively. Wave reflections, near field effects, wave directivity, and interference from P waves adds complexity and uncertainty in travel time determination in different orientations for experimental tests. In numerical simulations, the received waves did not require filtering and were mostly clean, with just minor P-wave interference. Received waves from both the experiments and the simulations exhibited an initial downward curve, following which the signal climbed up until it reached its peak value. The point at which this climbing signal first crossed the x-axis (often referred to as the first reversal) was taken as the time of arrival based on the recommendations in literature (Lee & Santamarina 2005, Cho et al. 2006, Ogino et al. 2015, Payan et al. 2016). It is noted the reported trends are not expected to change if a different method for determining arrival time is employed (Lee and Santamarina 2005). In Figures 3 and 4, arrows indicate the trigger times and interpreted arrival times. The travel distance was taken as the tip-to-tip distance between transmitting and receiving BEs. The shear wave velocity was the determined as the ratio of the tip-to-tip distance to the time of the first arrival. More details about the determination of travel time are presented in Basson et al. 2021.

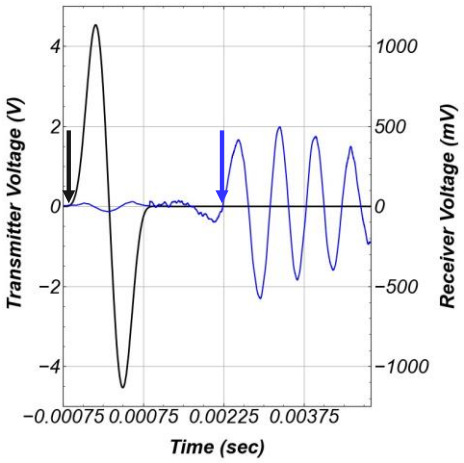

Figure 3. Transmitted (black) and received (blue) experimental signal for a VH wave transmitted through glass beads at 40 kPa isotropic stress. The time interval between the black and the blue arrows is taken as the travel time.

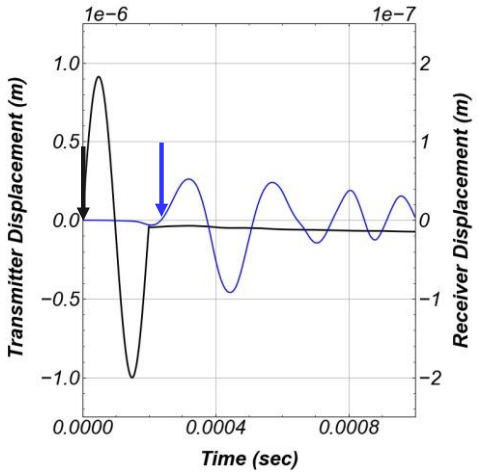

Figure 4. Transmitted (black) and received (blue) signal for a VH wave transmitted through spheres at 40 kPa isotropic stress.

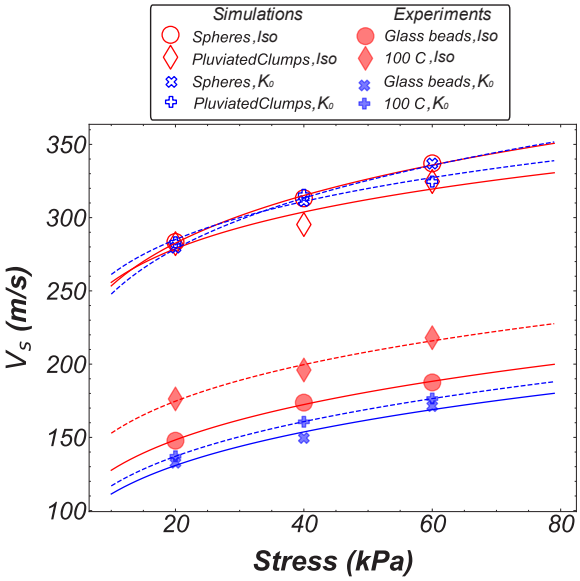

Figure 5. Increase in V_s with increase in confining stress for isotropic (black) and K_0 compression (gray).

3.2 *Influence of confining stress on Vs*

The increase in confining stress causes a change in the contact forces, which increases the contact stiffness and changes the fabric through particle rearrangement. Most relationships that have been proposed in the literature for describing the effect of confining stress on V_s have a power law form (Hardin & Richart 1963, Cascante & Santamarina 1996, Cho et al. 2006, Cha et al. 2014). The relationship with effective stress can be described is:

$$V_s = \alpha\,(\sigma_m')^{\beta} \tag{1}$$

where σ_m' is the mean effective stress in the polarization plane, α is the shear wave velocity at an effective confining stress of 1 kPa, and β is an exponent that captures the sensitivity of the skeletal shear stiffness to σ_m'.

The V_{VH} V_s measurements for the vertical BE pair follows the power law trend with mean stress for both experiments and simulations (Figure 5). As shown, the simulation results have a higher magnitude than the experimental results, which can be attributed to the higher stiffness of the simulated particles or to their larger size. This difference between experimental and numerical arrival times remains relatively unchanged if different signal interpretation methods are used. Additionally, variation in V_s magnitude due to stress conditions is smaller in simulation results than in experimental results, which could be attributed to

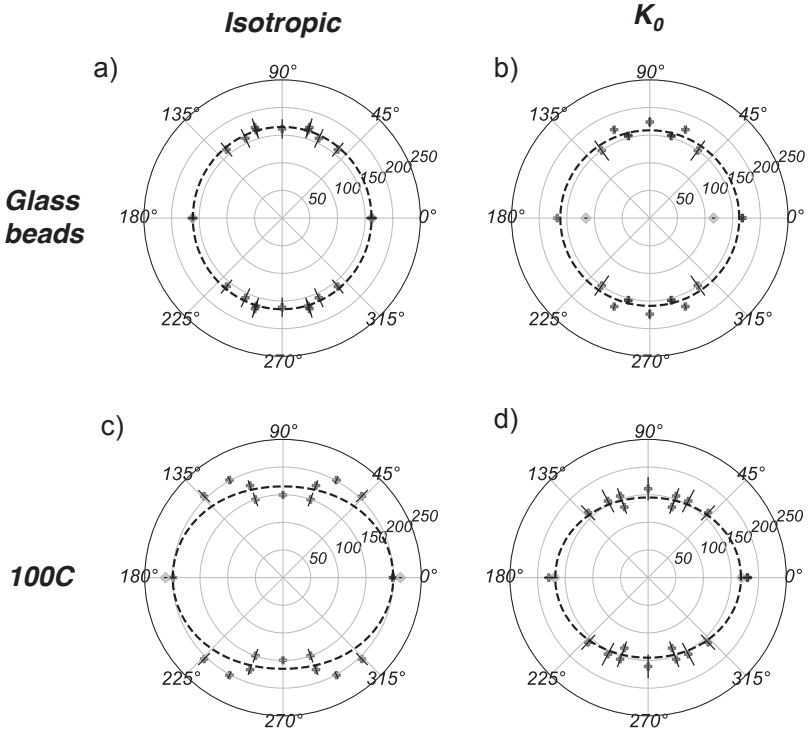

Figure 6 Polar plots of V_s for glass beads and 100C sand under isotropic and K_0 compression of 40 kPa; dashed line shows the best fit for VH to HV s weep. Black lines show the standard deviation for V_s measurements.

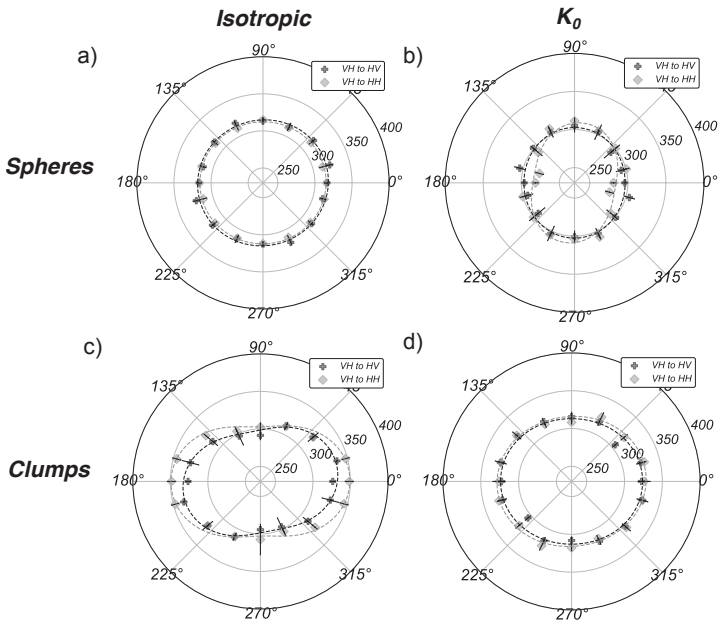

Figure 7. Polar plots of V_s for spheres and clumps under isotropic and K_0 compression of 40 kPa; dashed lines show the best fit for VH to HV and VH to HH sweeps. Black lines show the standard deviation for V_s measurements.

mean stress calculation accuracy. Namely, the various stress components are accurately measured in the DEM simulations mean stress for the specimen. Because the experiments did not allow for direct measurement of the horizontal effective stresses, a K_0 value of 0.5 was assumed for all the experiments.

3.3 Angular Variation of Vs

The angular distribution of V_s can be plotted using the measurements from the BE pairs at different orientations. This angular distribution is presented as a polar plot and is similar to the fabric polar plots. Based on the fabric polar plot fitting equations presented in literature (Rothenburg and Bathurst 1989, Mital et al. 2019, Basson & Martinez 2021), the angular distribution of V_s distribution can be fitted with an equation as follows:

$$V_s = V_{s,avg}\,(1 + a_{Vs}\,cos\,2\,(\theta - \theta_n)) \quad (2)$$

where $V_{s,avg}$ is the average V_s for a given mean effective stress, a_{Vs} is the magnitude of anisotropy in the distribution, and θ_n is the orientation from horizontal orientation with the maximum V_s value. An isotopic distribution would be circular with an anisotropy value of zero. In contrast, an anisotropic distribution would have a high a_{vs} and its shape would be like an elongated peanut. It is important to note that the polar plots were created assuming cross-anisotropy in the experimental and numerical specimen. This assumption holds true for the imposed stress conditions and shape of the specimen (Kuwano & Jardine 2002). Another way of quantifying anisotropy in V_s is by means of the V_{VH}/V_{HV} and V_{VH}/V_{HH} ratios, where a value greater than 1 denotes a greater V_s in the horizontal direction. A summary of different ratios and anisotropies is provided in Table 1 for specimens confined to mean stresses of 40 kPa.

The experimental polar V_s distribution for the glass beads and 100C sand compressed to 40 kPa in isotropic and K_0 conditions are shown in Figure 6. Figure 7 shows the DEM polar V_s distribution for VH to HV and VH to HH sweeps for spheres and clumps compressed under isotropic and K_0 conditions of 40 kPa. Due to the limitation of the experimental setup, only the VH to HV sweep was obtained. The polar plots for the glass beads and spheres specimen under isotropic compression resemble a circle because they are close to isotropic. The velocity ratios are 0.99 each for both experiments and simulations. The anisotropy values have small magnitudes, with a_{VHtoHV} value of 0.01 for the experiments and 0.0062 for the simulations, and a_{VHtoHH} value of 0.0044 for the simulations. For the glass beads under K_0 compression, the polar plot for the VH to HV sweep is close to circular, whereas the V_{HH} value is considerably smaller than the V_{VH} and V_{HV} values. The ratio V_{VH}/V_{HV} is 1.01 whereas the ratio V_{VH}/V_{HH} is 1.42. Similar results are observed for the DEM spheres under K_0 compression, where V_{VH}/V_{HV} is 1.03 and V_{VH}/V_{HH} is 1.10. Additionally, for the DEM simulations the a_{VHtoHH} is smaller (0.01) than a_{VHtoHH} (0.043). These trends can be explained by the stress conditions imposed under K_0 compression. For DEM simulations with sphere under K0 compression, vertical effective stress for spheres 54 kPa and the horizontal effective stress was 33 kPa, which produces a σ_m' of 43.5 kPa in the VH and HV direction and a lower σ_m' of 33 kPa in the HH direction. This difference in σ_m' increases the vertical stiffness of the specimen. Thus, the VH to HV sweep is unaffected by the increase in vertical stiffness, while the VH to HH sweep is affected.

Table 1. Summary of the results

Material	Stress condition	V_{VH} / V_{HV}	V_{VH} / V_{HH}	a_{VHtoHV}	a_{VHtoHH}
Glass beads	Iso	0.99	0.99	0.010	-
Glass beads	K_0	1.01	1.42	0.009	-
100C	Iso	0.75	0.71	0.094	-
100C	K_0	0.95	0.97	0.0172	-
Spheres	Iso	0.99	0.99	0.0062	0.0044
Spheres	K_0	1.03	1.10	0.010	0.043
Clumps	Iso	0.89	0.86	0.058	0.071
Clumps	K_0	0.97	0.94	0.017	0.020

Pluviation of angular particles under gravity causes the long axis of the particles to align with the horizontal direction (Oda 1972, Oda et al. 1982, Otsubo et al. 2020). For both the VH to HV sweep and the magnitude of V_{HH}, the fabric anisotropy generated by pluviation in a 100C specimen elongates the V_s polar plot in the horizontal direction for both isotropic stress cases. This is reflected in low V_{VH}/V_{HV} and V_{VH}/V_{HH} ratios of 0.75 and 0.71, respectively, which are in agreement with results from numerical and experimental results from Otsubo et al.

(2020) and Hamedani et al. (2021), along with an a_{VHtoHV} value of 0.094. The DEM simulations show similar results with V_{VH}/V_{HV} and V_{VH}/V_{HH} ratios of 0.89 and 0.86, respectively, along with an a_{VHtoHV} value of 0.058 and an a_{VHtoHV} value of 0.071. This indicates that the preferential orientation of particles developed during pluviation increases the horizontal stiffness.

The anisotropy in the horizontal direction of the 100C and clumps specimens compressed under K_0 conditions is significantly smaller than that of the isotropically compressed 100C and clumps specimens. For these specimens, there a competing mechanism between the induced vertical stress anisotropy due to the K_0 compression and the horizontal fabric anisotropy due to the pluviation. These two effects result in a decrease in anisotropy with respect to the isotropic stress case. The a_{VHtoHV} is of 0.0172 for experiments and of 0.017 for simulations, and a_{VHtoHH} is of 0.020 for the simulations. The velocity ratios are closer to 1.0 with respect to the isotropic stress values, with V_{VH}/V_{HV} and V_{VH}/V_{HH} of 0.95 and 0.97, respectively, for 100C, and of 0.97 and 0.94, respectively, for clumps. The experimental and numerical results show significant similarities in terms of the overall trends which suggest that V_s measurements can offer an indirect measurement of fabric and stress-induced anisotropy in soil specimens.

4 CONCLUSIONS

The effectiveness of employing anisotropy in shear wave velocity as an independent and indirect experimental estimation of fabric- and stress-induced anisotropy is addressed in this research. For both experimental tests and DEM simulations, wave propagation tests were conducted on various materials (spherical and angular/elongated) under varying magnitudes of stress in isotropic and K_0 conditions using a novel multi-bender element system. This multi-BE systems allows to measure V_s in varying directions and orientations. Curve fitting of the polar histograms of V_s versus direction angle, as well as the V_{VH}/V_{HV} and V_{VH}/V_{HH} ratios, were used to quantify anisotropy and preferential direction in the V_s distribution. Glass beads and spheres produced near isotropic V_s distributions under isotropic compression, whereas they produced a vertically elongated V_s distribution for VH to HH sweeps during K_0 compression. For 100C and clumps under isotropic compression, a horizontally elongated V_s distribution was produced for both the VH to HV and VH to HH sweeps. A competing mechanism between the stress induced- and fabric-induced anisotropy was observed and highlighted for 100C and clump particles under K_0 compression. Overall, the anisotropy in shear stiffness, which manifests in the directional variation of V_s, is influenced by particle shape, particle arrangement, contact behavior and stress conditions. This indirect methodology for estimating anisotropy may allow researchers to conduct more detailed investigations on the effect of fabric and stress on soil behavior and on the evolution of fabric during soil shearing.

5 ACKNOWLEDGEMENTS

This material is based upon work supported in part by the College of Engineering at the University of California Davis. The authors would like to thank Jasmine Miller for the assistance in experimental testing.

6 REFERENCES

Arulnathan, R., Boulanger, R. W., and Riemer, M. F. 1998. Analysis of Bender Element Tests, *Geotechnical Testing Journal,* Vol. 21, No. 2, pp. 120-131.

Basson, M. S., Martinez, A. 2020. A DEM Study of the Evolution of Fabric of Coarse Grained Materials during Oedometric and Isotropic Compression. *Proc. Geo-Congress 2020, Minneapolis, Minnesota, USA*.

Basson, M. S., Miller, J., Martinez, A. 2021. Experimental Estimation of Fabric in Granular Materials Using Shear Wave Velocity Measurements. *In Lecture Notes in Civil Engineering, Springer Singapore,* 311-323.

Cascante, G., Santamarina, J.C. 1996. Interparticle Contact Behavior and Wave Propagation. *Journal of Geotechnical Engineering.* 122, 831–839.

Cha, M., Santamarina, J.C., Kim, H.-S., Cho, G.-C. 2014. Small-Strain Stiffness, Shear-Wave Velocity, and Soil Compressibility. *Journal of Geotechnical and Geoenvironmental Engineering* 140, 06014011.

Cho, G.-C., Dodds, J., Santamarina, J.C. 2006. Particle Shape Effects on Packing Density, Stiff-ness, and Strength: Natural and Crushed Sands. *Journal of Geotechnical and Geoenvironmental Engineering*. 132, 591–602.

Geotechnique. 45.1.14

Hardin, B., Richart, F. 1965. Elastic Wave Velocities in Granular Soils. *Journal of Soil Mechanics and Foundation*

Kaviani-Hamedani, F., Kazem F., and Ali L. 2021. Bidirectional Shear Wave Velocity Measurements to Track Fabric Anisotropy Evolution of a Crushed Silica Sand during Shearing. *Journal of Geotechnical and Geoenvironmental Engineering* 147, no. 10-04021104.

Khalili. 2016. Small-Strain Stiffness of Sand Subjected to Stress Anisotropy. *Soil Dynamics and Earthquake Engineering* 88 (September) 143–51

Kuwano, R., and R. J. Jardine. 2002. On the Applicability of Cross-Anisotropic Elasticity to Granular Materials at Very Small Strains. *Géotechnique* 52 (10)

Lee, J.-S., Santamarina, J.C. 2005. Bender Elements: Performance and Signal Interpretation. *Journal of Geotechnical and 0020Geoenvironmental Engineering*, 131, 1063–1070.

Li, B., Zeng, X. 2014. Effects of fabric anisotropy on elastic shear modulus of granular soils. *Earthquake Engineering and Engineering Vibration*. 13, 269–278.

M. Aloufi, J. C. Santamarina. 1995. Low and High Strain Macrobehavior of Grain Masses: The Effect of Particle Eccentricity. *Transactions of the ASAE.* 38, 877–887.

Mital, U., Kawamoto, R., Andrade, J.E. 2019. Effect of fabric on shear wave velocity in granular soils. *Acta Geotechnica*.

Ning, Z. and T.M. Evans. 2013. Discrete Element Method Study of Shear Wave Propagation in Granular Soil. *Proc. of the 18 th International Conference on Soil Mechanics and Geotechnical Engineering, Paris, France*, pp. 1031-1034

Ning, Z., A. Khoubani, and T.M. Evans. 2015. Shear Wave Propagation in Granular Assemblies. *Computers and Geotechnics* 69 (September):615–26.

Oda, M., Konishi, S. Nemat-Nasser, S. 1982. Experimental micromechanical evaluation of strength of granular materials: Effects of particle rolling. *Mechanics of Materials*, 269-283.

Oda, Masanobu., 1972. Initial fabric and their relations to mechanical properties of granular materials. *Soils and Foundations*, 17-36.

O'Donovan, J., Ibraim, E., O'Sullivan, C., Hamlin, S., Muir Wood, D., Marketos, G. 2016. Micromechanics of seismic wave propagation in granular materials. *Granular Matter*. 18.

Ogino, T., Kawaguchi, T., Yamashita, S., Kawajiri, S. 2015. Measurement deviations for shear wave velocity of bender element test using time domain, cross-correlation, and frequency domain approaches. *Soils and Foundations.* 55, 329–342.

Otsubo, M, Junming Liu, Yuichiro Kawaguchi, Troyee Tanu Dutta, and Reiko Kuwano. 2020. Anisotropy of Elastic Wave Velocity Influenced by Particle Shape and Fabric Anisotropy under K Condition. *Computers and Geotechnics* 128 (December): 103775.

Otsubo, M., and Catherine O'Sullivan. 2018. Experimental and DEM Assessment of the Stress-Dependency of Surface Roughness Effects on Shear Modulus. *Soils and Foundations* 58 (3): 602–14.

Payan, Meghdad, Arman Khoshghalb, Kostas Senetakis, and Nasser

Roesler, S.K. 1979. Anisotropic shear modulus due to stress anisotropy. *J. Geotech. Eng*. Div. ASCE.

Rothenburg, L, and R. J. Bathurst. 1989. Analytical Study of Induced Anisotropy in Idealized Granular Materials. *Geotechnique*, 39-4, 601-614.

Stokoe, K. H., II, and Santamarina, J. C. 2006. Seismic wave based testing in geotechnical engineering. *Proc. in International Conference on Geotechnical and Geological Engineering*, 1490-1536.

Sturm, A. 2019. On the Liquefaction Potential of Gravelly Soils: Characterization, Triggering and Performance. *Ph.D. thesis UC Davis.*

Viggiani, G., Atkinson, J.H.: 1995. Interpretation of bender element tests.